Military Technical College
Kobry El-Kobbah,
Cairo, Egypt.

17th International Conference on Applied Mechanics and Mechanical Engineering.

CHARACTERIZATION OF CLOSED-CELL ALUMINUM FOAMS PRODUCED BY MELT-BASED TECHNIQUE

H. A. Afifi[1], M. H. Ahmed[2] and I. M. El-Galy[3]

ABSTRACT

Metal foams are interesting materials; not only for their metallic constituents, but also for the characteristics gained by the voids distribution. Metal foams find increasingly more applications in several industrial applications due to their novel physical, mechanical, thermal, electrical and acoustic properties. The high specific strength or stiffness in conjunction with distinct functional properties make them potential material for light-weight construction, energy and sound absorption applications.

This investigation focuses on the parameters affecting the foaming process of aluminum based on $CaCO_3$ as an economical foaming agent. The foaming parameters (e.g. percentage of the foaming agent, stirring speed and time, pre-foaming temperature) are decisive in controlling the resulting foam structure. The physical and mechanical properties of the resultant foam could be correlated to the different foaming parameters. The addition of aluminum and Al_2O_3 powder to the melt showed a remarkable improvement in the characteristics of the produced foam.

KEY WORDS

Aluminum, Foam, Closed-Cell, $CaCO_3$, Blowing Agent, Energy Absorption

[1] Research Assistant, Production Engineering Dept., Alexandria University, Egypt.
[2] Associate Professor, Production Engineering Dept., Alexandria University, Egypt.
[3] Assistant Professor, Production Engineering Dept., Alexandria University, Egypt.
Corresponding author: i_elgaly@alexu.edu.eg.

INTRODUCTION

Cellular materials are widespread in everyday life and are used in civil and mechanical construction for damping, insulating, impact cushioning, filling, and filtering purposes as well as many other applications. Highly porous materials possess high stiffness to weight ratio, which make them attractive for lightweight structures and energy saving purposes. The term foam is usually reserved for dispersion of gas bubbles in a liquid. The morphology of such foam can be preserved by letting the liquid solidify, thus obtaining what is called *Solid Foam* [1]. Foams can be also classified according to their cellular structure into open-cell and closed-cell structures as shown in Fig. 1 [2]. Over the last decades, many efforts have been made to foam different polymers, glasses, ceramics, and metals to produce porous structures [3]. Metallic foams are finding an increasing use in light weight applications ranging from automotive, construction and ship building industries to decorative applications, medical and sports equipment [4].

A wide range of processes are used to produce metallic foams, ranging from general foaming techniques applicable to almost any metal, to specialized and highly specific processes. These processes differ in the nature of the foams produced, as well as the ease of processing, the degree to which control can be obtained over the foam structure by adjusting process parameters, and the potential for adapting the processes to rapid and cost-effective industrial production.

The objective of the current work is to investigate the parameters affecting the production of aluminum foams using a melt-based technique with the aid of powder blowing agent. By testing the physical and mechanical properties of the foam produced under different foaming conditions, the effects of the different parameters can be determined, so that the characteristics of the required foam can be tailored. Moreover, the viability of using $CaCO_3$ powder as a foaming agent can be proven.

PRODUCTION TECHNIQUES OF CLOSED-CELL METALLIC FOAMS

One of the first ever reported evidences of metal foam was published by Meller in 1926 [5], where foaming of light metals (e.g. aluminum and its alloys) either by inert gas injection or by using a blowing agent (e.g. carbonate and bicarbonate) was suggested. In 1948 and later in 1951, Sosnick patented a technique to produce foamed aluminum by vaporization of mercury in molten aluminum [6], [7]. Subsequently, Elliott brought the idea of adding TiH_2 as a blowing agent to the molten aluminum alloys to produce metal foams [8]. The blowing agent may be mixed with metal powders instead of molten metal. This was realized by Pashak in 1960 [9]. However, the mixture must be extruded and heat treated to produce foam.

The process was further developed by Allen et al. [10], who used TiH_2 and $CaCO_3$ as blowing agents. Copper, nickel and zinc alloys were foamed by Niebylski et al. [11]. They showed that stirring during addition of the blowing agent resulted in a more uniform structure. In 1976, Speed investigated the pretreatment of the metal hydride and the control of decomposition start [12]. Shinko Wire Company (Japan) developed a new commercial process, in which Ca, $CaCO_3$ and TiH_2 are stirred with aluminum melt [13]. Further developments included the foaming of metallic matrix composites.

Foaming by gas injection was explored in 1990s at Alcan (Montreal, Canada) [14]. The introduction of gas into a metallic composite (containing ceramic particles) generates foam at the surface of the melt. This process is currently being exploited by Cymat Technologies in Canada. A new concept of gas injection that leads to foams with excellent uniformity of cell sizes was developed in Kleinreichenbach, (Austria) [15]. By casting the foam into moulds, complex-shaped foamed parts can be manufactured. This type of foam is called Metcomb.

The production based on metal powder and blowing agent as starting materials was brought to sophistication at Fraunhofer-Institute in Bremen (Germany) by Baumeister [16]. This process is known today as powder metallurgical or PM route of metal foam production. With the beginning of the 21st century, the advantages of melt- and PM-route approaches have been combined in a new processing technique known as FORMGRIP [17]. It involves preparation of a precursor material by dispersion of gas-generating particles in a liquid aluminum-based composite, followed by solidification. Subsequent heating of this precursor results into a closed-cell foam.

CHARACTERISTICS OF CLOSED-CELL METALLIC FOAMS

The most important properties for closed-cell aluminum foams are their elastic stiffness, their collapse strength and the 'plateau' stress (i.e., the value of stress at which the cells have completely crushed and collapsed). These mechanical properties are mainly influenced by the density of the produced foam [18]. Mechanical properties of foam have been investigated by many researchers. Deqing and Weiwei [19] have investigated the relationships between compressive properties and cell structures of the closed-cell aluminum foams and found that the plastic collapse strength and energy absorption capacity of the closed cell aluminum foams are significantly improved by reducing the cell size of foams having the same density. As an energy-absorbing material, foams have the characteristics that higher strain could be obtained at lower stress levels. According to Gibson and Ashby [2], the energy absorption capacity of closed-cell Al foam depends upon the plateau stress (equation 1). The higher the foam's yield stress, the greater the energy absorbed.

$$W = \int_{\varepsilon 1}^{\varepsilon 2} \sigma_{pl}\, d\varepsilon \qquad (1)$$

where, W is the energy absorption capacity and σ_{pl} is the plateau stress.

Ramamurty and Paul [20] examined the variability in elastic modulus, plastic strength, and energy absorption of closed-cell Al foam, and correlated the mechanical properties of the investigated "ALPORAS" foam to its relative density. Peroni [21] studied the mechanical properties of Al foams with different densities and found that higher density foams are more anisotropic. The collapse strength and the absorbed energy increase with density, too. The influence of structural properties on the mechanical properties of closed-cell Al foams was also studied by Idris et al. [22], Raj and Daniel [23]. Peixinho et al. [24] characterized the crash properties of Al foams. Haesche et al. studied the effect of replacement of TiH_2 as foaming agent by $CaCO_3$ in production of aluminum foam and found that the maximum energy absorption capacity is achieved in foams with the lowest relative density [25].

EXPERIMENTAL WORK

Aim of the experimental work is to achieve a controlled foam structure with preset properties. The blowing agent technique has been used for the production of the aluminum foam as illustrated schematically in Fig. 2. Calcium carbonate has been selected as the blowing agent because it has been found to be a highly effective foaming agent for aluminum [3], [25]. The chemical decomposition of $CaCO_3$ is more gradual at the aluminum melting temperature. This improves the control over the foaming process, while the extremely low material cost, non-hazardous nature of the foaming agent and the decomposition products are favorable.

Investigated production parameters included the percentage of blowing agent, the stirring speed and duration, the pre-foaming temperature and the foaming duration. During the foam production, the metal is heated to 750ºC, 800ºC and 850ºC using electrical resistance furnace. Temperature measurements were carried out using a K-type thermocouple located in the melt crucible. After melting, $CaCO_3$ powder was added to the melt as a percentage of the melt weight. The amount of carbonate added to the melt was selected based on the values mentioned in the literature in the range of 2 to 4% of the base metal mass. A steel stirrer has been used to disperse the foaming agent at different stirring speeds ranging from 460 to 1280 rpm.

Because $CaCO_3$ cannot be easily wetted by molten aluminum, the dispersion of the foaming agents in the metal melt can be assisted by adding aluminum powder as a stirring agent that can be mixed with $CaCO_3$ prior to its addition to the melt [1]. A mass ratio of (1x$CaCO_3$: 2xAluminum Powder) was found to be sufficient to disperse the carbonate powder. The mixture of powders is introduced to the melt and dispersed by stirring for a duration ranging from 1 to 2 minutes. The mix is allowed to foam for duration between 4 and 10 minutes before it is forced to solidify by quenching in water. The different levels of foaming parameters are shown in Table 1. “Taguchi Method” for experimental design [26] has been applied with orthogonal arrays to determine the combination of parameters and the interaction between the different parameters. All experiments have been performed according to this design.

The weights and volumes of the foam samples were determined before they were sectioned. The sections were embedded in epoxy resin to facilitate grinding and polishing without affecting the cell structure. Pore sizes have been evaluated with the aid of stereo-microscope and image analysis software. The whole sample cross section was divided into 9 equal zones for the purpose of analysis as shown in Fig. 3. To evaluate the compressive strength of the produced foam, cubic samples with (20x20x20 mm^3) have been cut from the middle region of the foamed block. Compression tests were carried out on a 30 ton Schimadzu universal testing machine at a speed of 0.3 mm/min.

RESULTS AND DISCUSSION

As mentioned earlier, density plays an important role in defining the mechanical characteristics of foams. Taguchi analysis has been applied to determine the most important factor among the different production parameters that affects density of the produced foam. According to Taguchi method [26], the signal-to-noise ratio, or the *SN*

number (Equation 2) is calculated for each experiment within the predefined orthogonal L18 arrays:

$$SN_i = 10\,log\,\frac{\overline{Y_i}^{\,2}}{{S_i}^2} \qquad (2)$$

where:

$${S_i}^2 = \frac{1}{N_i - 1}\sum_{u=1}^{N_i}(U_{i,u} - \overline{Y_i})^2 \quad \text{and} \quad \overline{Y_i} = \frac{1}{N_i}\sum_{u=1}^{N_i} Y_{i,u}$$

$\overline{Y_i}$ = The mean value of the results
S_i = The variance
i = Experiment number (1, 2, 3, …., total number of experiments)
u = Trial number (1, 2, …, N_i)
N_i = Number of trials for experiment *i*.
$Y_{i,u}$ = The results of the experiment for each combination

After calculating the *SN* ratio for each experiment, the average *SN* values must be calculated for each level inside each factor. The range *R* : (*R* = high*SN* - low*SN*) for each parameter is calculated. The larger the *R* value for a parameter, the larger the effect the variable has on the process [26].

The result is shown in Fig. 4 indicates that the stirring speed and the percentage of $CaCO_3$ are the most influencing parameters on the foam density. The nature of these effects will be represented later. The same analysis has been applied to the average cell size of the produced foam to investigate the most significant or affecting factors. It is obvious from Fig. 5 that the melting temperature is the most effective factor on the cell size. This may be interpreted by the effect of the temperature on the viscosity of the molten media, which strongly controls the expansion of the bubbles during the foaming process.

Effect of Processing Parameters on the Physical Properties of Foam

Effect of the percentage of foaming agent

In order to determine the optimum weight percentage of $CaCO_3$, in addition to the influence of varying this amount on the properties of the produced foam, a number of experiments have been performed using 2%, 3% & 4% wt of $CaCO_3$. Other parameters were kept constant (stirring speed 730 rpm, stirring duration 1 min., pre-foaming temperature 800 ℃ and foaming duration 10 min.). As shown in Fig. 6, the relation between the determined relative density for each sample and the % of $CaCO_3$ is not linear. It is not always true that increasing percentage of foaming agent will result in more foaming and less density, but there is a maximum limit, after which an excessive amount of foaming agent is detrimental. Increasing the amount of released gases may lead to thinning in the walls between neighboring cells and collapsing.

The relation between the average cell size of the produced foam and the percentage of $CaCO_3$ is represented in Fig. 7. The maximum expansion of cells occurs with 3% $CaCO_3$, while the lowest expansion was recorded at 1% $CaCO_3$. With 4% $CaCO_3$ the cells start to collapse due to the excessive amount of $CaCO_3$. It should be noticed, that some tests have been performed at levels higher or lower than the pre-specified values to verify the fitness of the selected ranges.

Effect of the stirring speed

The stirrer speed is another important parameter, that affects the success of foaming process since it affects the dispersion of the foaming agent inside the molten metal. A number of speeds (460, 730 and 1280 rpm) have been used to determine the optimum speed. Fig. 8 shows the relation between stirring speed and the density of the foam. An inverse relation between stirring speed and foam density was observed. The reduction in the relative density was 20% when the speed increased from 460 to 730 rpm, although the reduction was 10% when the speed increased from 730 to 1280 rpm. The percentage of reduction in density is lowered with increasing the stirring speed. This could be due to thinning and collapsing of cell walls caused by the additional air entrapment that takes place at high stirring speed.

The relation between stirring speed and the average cell size of the produced foam is shown in Fig. 9. The cell size has been increased by about 40% by increasing the stirring speed from 460 to 730 rpm, while increasing the speed to 1280 rpm resulted in a slight increase of about 5% caused by increased collapse of the cells.

Effect of the stirring duration

The nature of the effect of stirring duration on density is represented in Fig. 10. A stirring duration of 1.5 minute has been found to be suitable to achieve complete mixing of the powder with the aluminum mass. Increasing the stirring duration beyond 1.5 minute did not show obvious reduction of foam relative density, while affecting the foaming duration negatively. Increase of stirring duration shortens the duration available for foaming before complete solidification. Generally, increasing the stirring duration behind a certain level results in solidification of the melt and/or collapse of the foam. While a very short stirring duration will not be sufficient to complete the powder dispersion.

The effect of stirring duration on the average cell size of the produced foam is shown in Fig. 11. The cell size increases by increasing the stirring duration. The prolonged stirring gives more time for the generated bubbles expand. This expansion can lead to coalescence of walls between neighbor cells generating larger ones. It can be concluded that further increase of stirring speed or time leads to spattering of the molten metal, increased cooling rates and destruction of generated cells.

Effect of the pre-foaming temperature

In Fig. 12 the relation between pre-foaming temperature and the relative density is shown. It is obvious that increasing the temperature from 750 to 850 ℃, decreased the relative density from 26.8% to 20.2%. Any further increase of temperature above 850℃ is not preferable, since it results in reducing the viscosity of the molten metal, and that will help the deformed bubbles to escape to the surface before the solidification occurs.

The relation between pre-foaming temperature and the average cell size is shown in Fig. 13. The cell size increased by nearly 50% as the temperature increased from 750 to 800 ℃, while increasing the temperature to 850 ℃ led to an increase in the average cell size by only 15%. That could be interpreted by the effect of temperature rise on reducing the viscosity of the molten metal, which in turn affects the ability of cell to retain its shape and size during foaming or expansion.

Effect of the foaming duration

Foaming duration is the time through which foaming takes place, it is not preferable to give this step very long or very short foaming duration to prevent undesirable side effect of the produced structure(i.e. drainage effect, cell collapsing, and coalescence of neighboring cells), the suitable range of foaming duration is between 1 and 15 minutes. In Fig. 14 and Fig. 15 three values (4, 7 and 10 min.) were chosen to determine the effect of foaming duration on the density and pore size of the foam.

Mechanical Characterization of the Produced Foam

The objective of the mechanical testing is to correlate the mechanical properties of the produced foam to the physical properties (relative density, pore size and percentage of defects). Since the most important property of metallic foams is their ability to absorb large amounts of energy in compressive plastic deformation [3]. Samples of the produced foams were sectioned using a low speed saw to prepare cubic specimens (20x20x20 mm^3) for compression testing. Specimens were uniaxially compressed at a constant speed of 0.3 mm/min using a universal testing machine equipped with parallel plates. The plates were lubricated with hydraulic oil before the tests. The samples were grouped into two sets according to the sample densities and pore sizes.

In order to determine the influence of the foam density on the output mechanical properties of the foam, three samples were selected, these samples have almost the same average pore diameter but with different density. The stress strain curves for three samples with different relative densities (i.e. 13.7, 17.4, and 26.6%) are shown in Fig. 16. The compressive behavior of the aluminum foam goes through three stages: an elastic deformation stage, followed by a plastic deformation stage both combined with densification of the foam structure. A high gradient rise in strength is observed when high densification levels are reached. The nearly constant plateau stress starts at the phase in which the collapse of the cells emerges. The cells start to bend and extend or contract, while the membranes which form the cell faces stretch. This increases the contribution of the axial cell wall stiffness. If the membranes do not rupture, the compression of the gas in the cells also increases their stiffness. After opposing cell walls touch, further strain compresses the solid itself giving the final region of steeply increasing stress, referred to as densification, with a slope approaching the young modulus of the solid metal. It is observed that the plateau stress increases with increasing the relative density (i.e. decreasing porosity), while the densification stage emerges nearly at 58% strain. It is noticed that the densification strain is retarded in foams with increasing the foam density. This trend confirms the findings of Koza et al. [27]. It is interesting that the lightest foam (relative density of 13.7%) achieved a compressive strength higher than that of heavier foams after 50% strain.

In addition to relative density, average cell size influences the mechanical properties of the foam. Fig. 17 represents the compression stress-strain curve for three samples with different average cell size all having 26.6 % relative density. It is obvious that the plateau stress is about 8.2 MPa when the pore size is about 3.96 mm; and the plateau stress is nearly 6 MPa when the pore size is about 4.65mm; while it is lowered to nearly 4 MPa when the produced pore size is 6.05 mm. For foams having similar pore size, the higher the density, the thicker is the pore cell wall; so the foam can bear a higher

load giving a higher stress plateau. For foams having similar density, the larger the pore size, the lower the plateau stress. This confirms the findings in [18]. It is very useful to notice that the rise of strength takes the same trend or gradient independent of the pore size, while the strain at which the foam cells have totally collapsed (densification strain) will be retarded with increasing the pore size. The results of Fig. 16 and Fig. 17 mean that the energy absorption varies with the variation of both the relative density and average pore size. The relationship between the energy absorption capability of the specimen of different densities and selected strain region is shown in Fig. 18. The energy absorption capability has been estimated by the following equation (3):

$$W = \int_0^{\varepsilon} \sigma(\varepsilon)\, d\varepsilon = \sum_{i=1}^{n} \sigma_i \varepsilon_i \qquad (3)$$

where, W is the energy absorbed by foamed metal; σ the stress and ε the strain in the compression test, $d\varepsilon$ is the densification strain at which all cells in the structure have collapsed. It can be seen that the energy absorption capability of the aluminum foam is much higher than that of the solid aluminum. This is true for all stress levels below the stress necessary to reach the foam densification strain. The solid metal is still loaded in the elastic region, while the collapse of the foam cells absorbs a large amount of energy. Comparison of foams with different densities (Fig. 18) shows that foams with higher relative density can offer minimum amount of deformation at the same level of energy absorption. It is also possible to realize a specific level of energy absorption with foams having different relative densities.

Besides relative density and cell size, specific strength of foams represents a very important aspect. Fig. 19 shows the specific stress vs. strain curve for two samples made from aluminum solid (σ_y = 60 MPa, ρ_s = 2.7gm/cm^3) and metal foam ($\sigma_{plat.}$ = 8.2 MPa, ρ_f = 0.67 gm/cm^3). The strength ratio of the plateau strength of foamed metal to the solid aluminum is 0.137, while comparison of strength to weight ratio shows a clear improvement in favor of the foam structure. The specific strength of foamed aluminum to that of solid is 0.551, where $\sigma_{plat.}/\rho_f$ = 12.24 for the foamed aluminum and $\sigma_{y.}/\rho_s$ = 22.22 for the solid aluminum.

Microstructural Examination

Random samples of aluminum foam have been examined under Axiovert microscope with magnification 500X to investigate the inner surface of the cells. Oxides (e.g. Al_2O_3) have been observed in these samples (Fig. 20). Two probable sources of these oxide films; the first of which is carbon dioxide which results from the decomposition of $CaCO_3$. The second source is the amount of air that inserted into the molten metal during the stirring process. The aluminum oxide forms layers at the inner surface of the aluminum cells. The thickness of these layers depends on the amount of the oxidizing gases inside each cell. These layers have a significant influence on the size and shape of the foam cells. A heterogeneous structure is also observed due to the existence of inter-metallic compound ($TiAl_3$).

The three microstructures shown in Fig. 21, reveal variation in the size of the spheroids (micro-cells) and grains produced with different amounts of $CaCO_3$. As the amount of

$CaCO_3$ increases, a thicker oxide layer is formed resisting the expansion of the cells and results in reduced spheroids size.

CONCLUSION

1. Production of aluminum foams using $CaCO_3$ as a foaming agent represents a cost effective production method within the specified characteristics range.
2. The physical characteristics of the produced foam can be tailored to meet the mechanical loading requirements by adjusting the processing parameters (i.e. stirring speed, % of the foaming agent, foaming duration, stirring duration, and pre-foaming temperature).
3. The lightest foam (density=0.34 gm/cm^3) could be obtained under the following conditions: Pure aluminum as a base metal, $T = 850\,^{\circ}C$; $CaCO_3$ = 3% of aluminum weight; 2% Al powder; stirring speed = 1280 rpm; stirring duration = 1 min. and foaming duration = 10 min.
4. The high densification phase is clearly observed beyond 58% strain.
5. The behavior of the produced foams under compression as well as their energy absorption capacity shows a high degree of dependency on the physical properties, especially, the relative density and the average pore diameter.
6. Up to the densification strain, the energy absorption capacity of the produced foam is much higher than that of the solid aluminum. This makes it attractive structural element for impact and vibration applications.
7. Foaming of aluminum improves the specific strength. The strength ratio of the plateau strength of foamed metal to the solid aluminum is 0.137, while the specific strength of foamed aluminum to that of solid is 0.551.

ACKNOWLEDGMENT

The authors would like to thank the materials technology labs at Alexandria National Steel – Dekhila (ANSDK) for supporting the mechanical testing part of this work.

REFERENCES

[1] C. Koerner, "Integral Foam Molding of Light Metals", Univ. Erlangen-Nürnberg, Germany, 2008.
[2] L. J. Gibson, M. F. Ashby, "Cellular Solids: Structure and Properties". 2nd edition, Cambridge University Press, 1997.
[3] D. C. Curran, "Aluminium Foam Production using Calcium Carbonate as a Foaming Agent", PhD Dissertation, University of Cambridge, U.K., 2003.
[4] C. Kammer, "Aluminium foam", European Alum. Association, Germany, 1999.
[5] M. A. De Meller, French Patent 615,147, 1926.
[6] B. Sosnick, US Patent 2,434,775, 1948.
[7] B. Sosnick, US Patent 2,553,016, 1951.
[8] J. C. Elliott, US Patent 2,983,597, 1961.

[9] J. F. Pashak, US Patent 2,935,396, 1960.
[10] B. C. Allen, M. W. Mote, A. M. Sabroff, US Patent 3,087,807, 1963.
[11] L. M. Niebylski, C.P. Jarema, US Patent 3,847,591, 1974.
[12] S. E. Speed, US Patent 3,981,720, 1976.
[13] S. Akiyama, et al., US Patent 4,713,277, 1987.
[14] I. Jin, L. D. Kenny, H. Sang, US Patent 4,973,358, 1990.
[15] D. Leitlmeier, H. P. Degischer, H. J. Flankl, "Development of a Foaming Process for Particulate Reinforced Aluminum Melts", Advanced Engineering Materials, 2002, 4: p. 735-740.
[17] J. Baumeister, German Patent 4,018,360, 1991.
[18] V. Gergely, B. Clyne, "The FORMGRIP Process: Foaming of Reinforced Metals by Gas Release in Precursors", Advanced Eng. Materials, 2000, 2: p. 175-178
[19] W. Peng, L. Lin, "Influence of Density on Compressive Properties and Energy Absorption of Foamed Aluminum Alloy", Journal of Wuhan University of Technology-Mater.Sci. Ed. June 2007.
[20] W. Deqing, X. Weiwei, M. Xiangjun, S. Ziyuan , "Cell structure and compressive behavior of an aluminum foam", J. of Materials Science, 40, 2005, 3475 – 3480.
[21] U. Ramamurty, A. Paul, "Variability in Mechanical Properties of a Metal Foam", Department of Metallurgy, Indian Institute of Science, Bangalore 560012, India, Elsevier Publisher, October 2003.
[22] L. Peroni, M. Avalle," The mechanical behaviour of aluminium foam structures in different loading conditions, International Journal of Impact Engineering 35 (2008) 644–658.
[23] M. I. Idris, T. Vodenitcharova, M. Hoffman, "Mechanical behaviour and energy absorption of closed-cell aluminium foam panels in uniaxial compression", Elsevier Publisher, March 2009.
[24] R. Edwin Raj, B.S.S. Daniel, "Structural and compressive property correlation of closed-cell aluminum foam", J. of Alloys and Compounds 467 (2009) 550-556.
[25] N. Peixinho1, P. Pinto1, F. Silva1, D. Soares, "Crash Energy Absorption Of Aluminium Foams With Modified Cellular Structures", Center for Materials and Mechanical Techn., Univer. do Minho, Guimarães, Portugal, 2013.
[26] M. Haesche, D. Lehmhus, M. Wichmann, I. C. Mocellin, "Carbonates as Foaming Agent in Chip-based Aluminium Foam Precursor", Elsevier, 2010.
[27] E. B. Dean," Taguchi Approach To Design Optimization for Quality and Cost", Annual Conference of the International Society of Parametric Analysis, 1991.
[28] E. Koza, M. Leonowicz, S. Wojciechowski, F. Simancik, "Compressive Strength of Aluminium Foams", Faculty of Materials Science and Engineering, Warsaw University of Technology, Woloska 141, 02-507 Warsaw, Poland Institute of Materials and Machine Mechanics, Slovak Academy of Sciences, Poland, 2003.

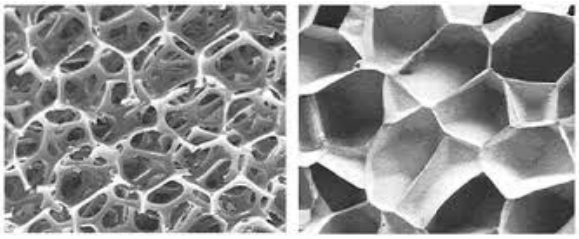

Fig. 1. Open-cell and closed-cell types of metal foam structures [2].

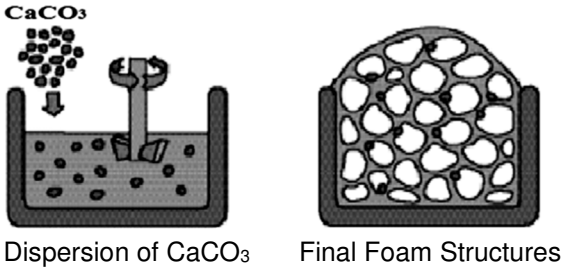

Fig. 2. Illustration of foam production steps using $CaCO_3$ [3].

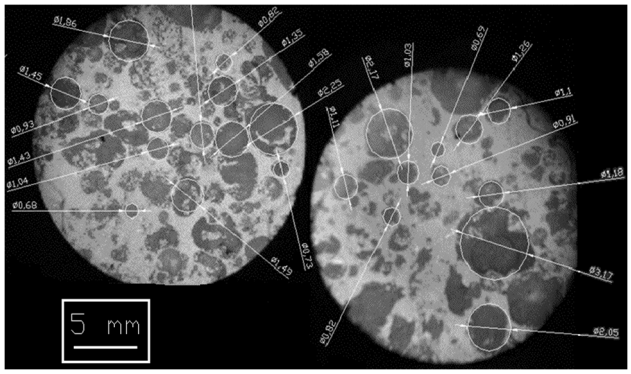

Fig. 3. Examples of cell size evaluation for typical zones.

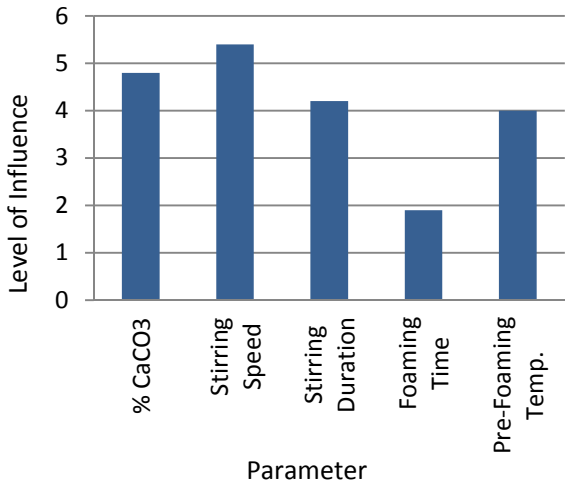

Fig. 4. Ranking of the processing parameters affecting foam density.

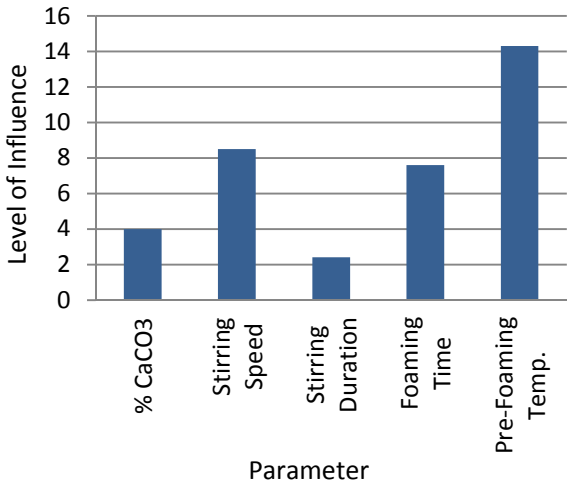

Fig. 5. Ranking of processing parameters affecting average cell size.

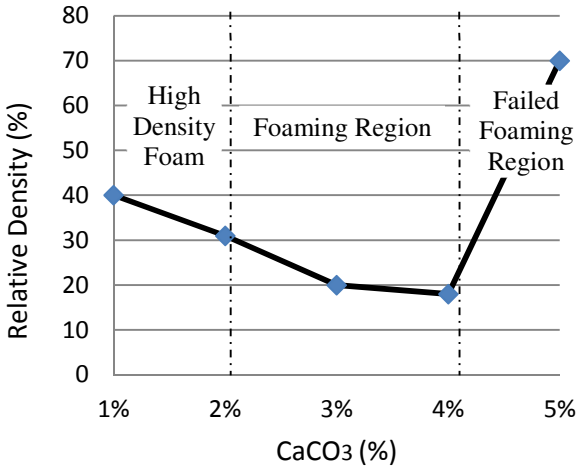

Fig. 6. Effect of varying the % of $CaCO_3$ on the % of relative density.

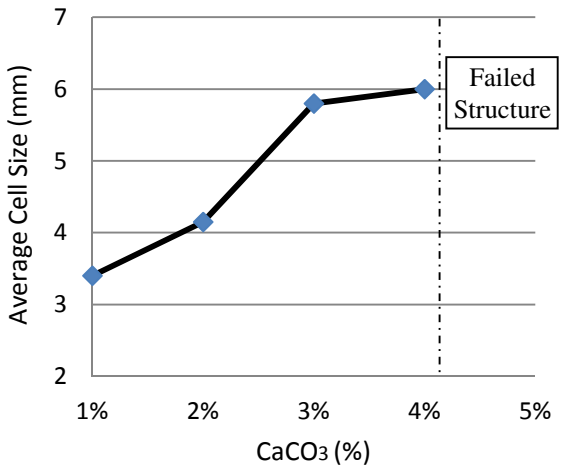

Fig. 7. Effect of varying the % of $CaCO_3$ on the average cell size.

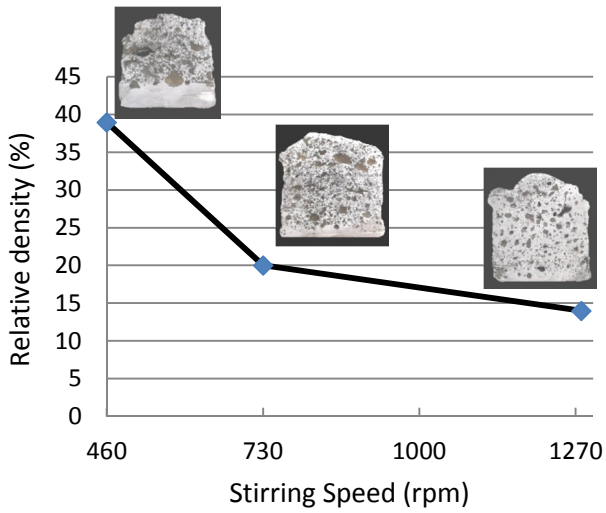

Fig. 8. Relation between stirring speed and the density of the produced foam.

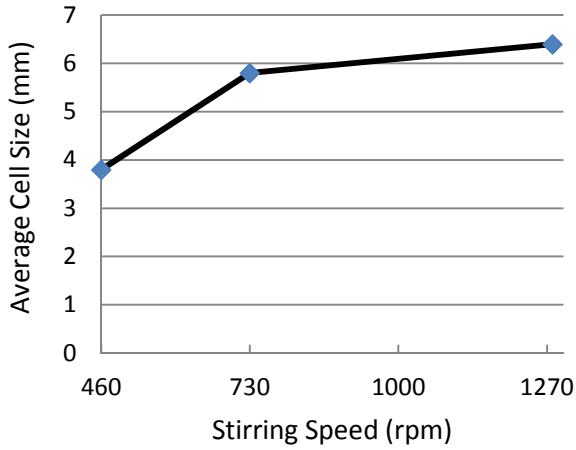

Fig. 9. Relation between stirring speed and average cell size.

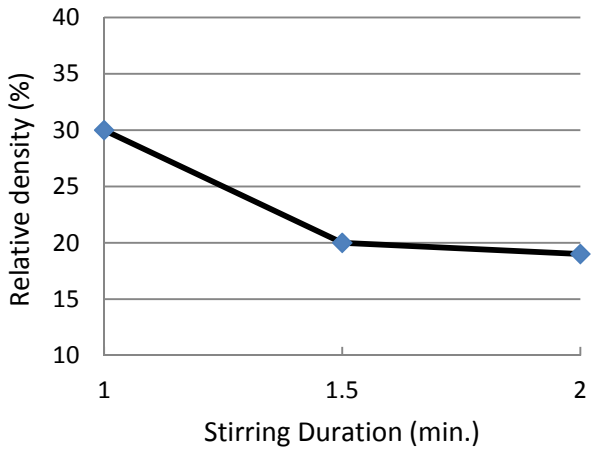

Fig. 10. Relation between stirring duration and the density of the produced foam.

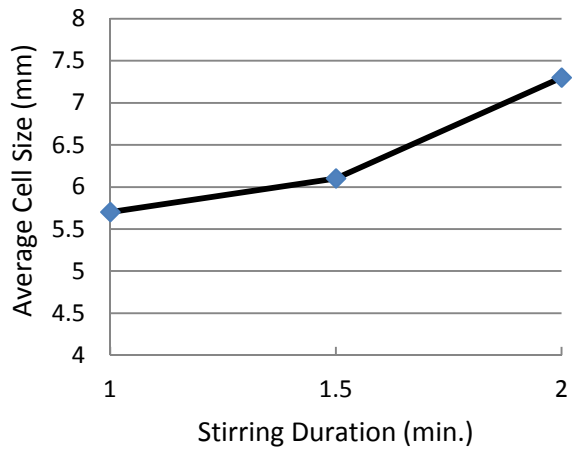

Fig. 11. Relation between stirring duration and average cell size.

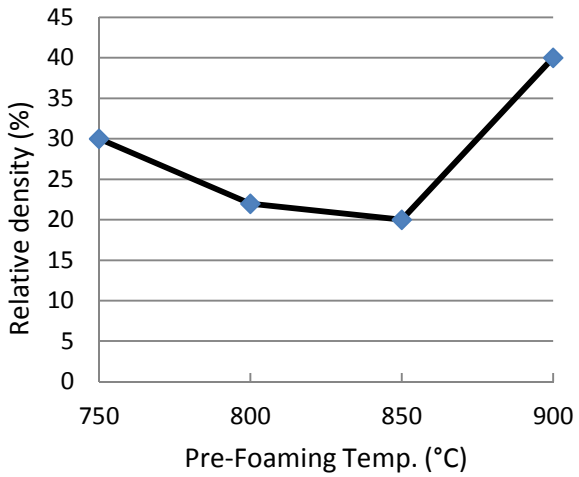

Fig. 12. Relation between pre-foaming temperature and density of foam.

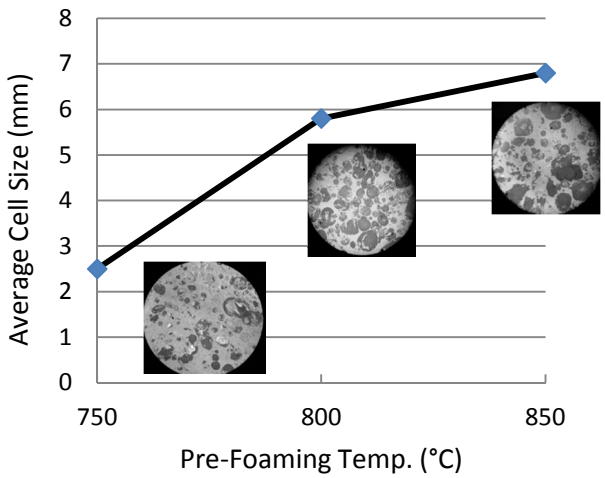

Fig. 13. Relation between pre-foaming temperature and average cell size.

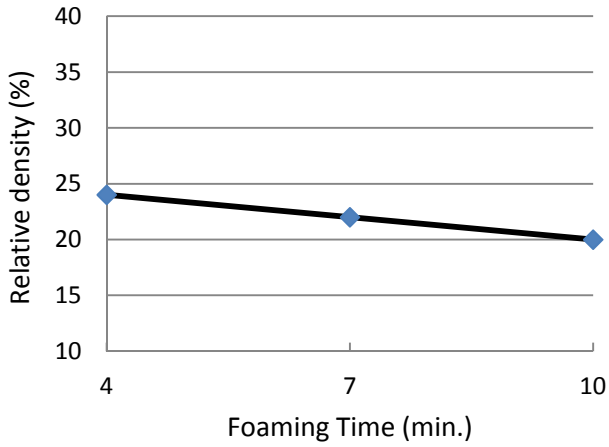

Fig. 14. Relation between foaming duration and the density of the produced foam.

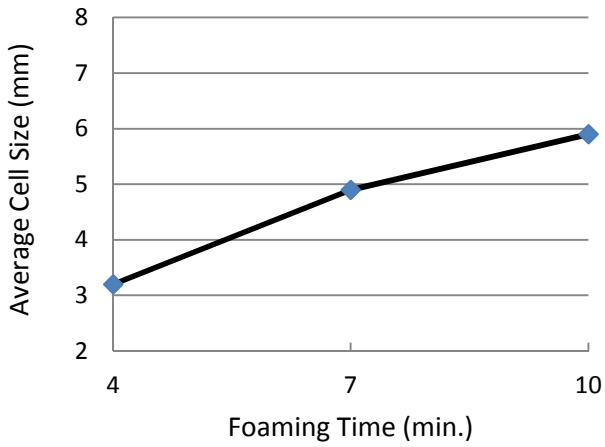

Fig. 15. Relation between foaming duration and average cell size.

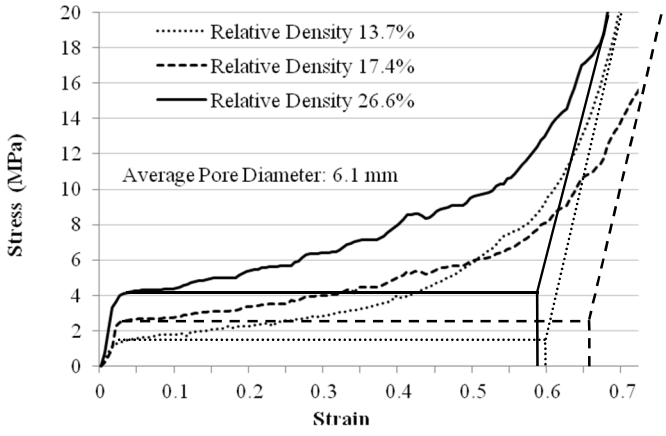

Fig. 16. Stress strain curves for samples having the same pore size but different densities.

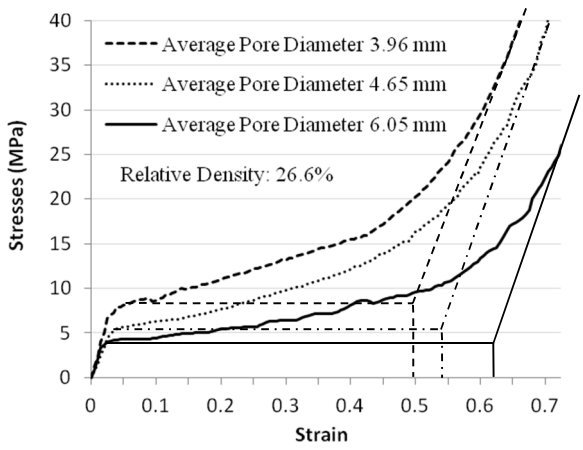

Fig. 17. Stress strain curves for samples having the same density but different pore size.

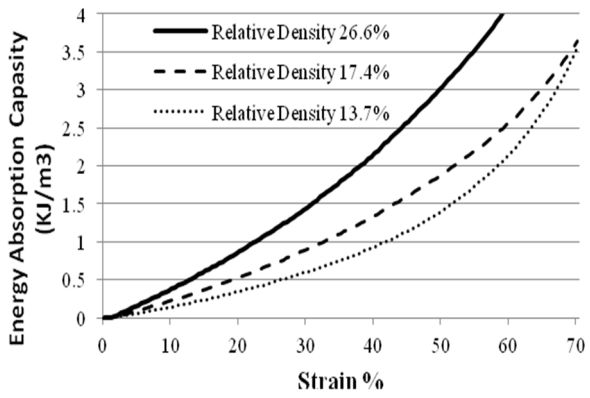

Fig. 18. Energy absorption capabilities of specimens having different densities.

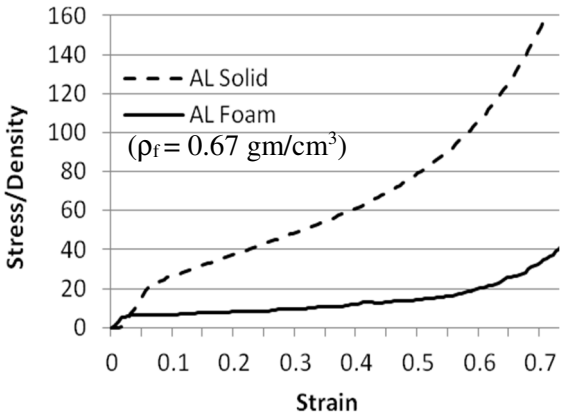

Fig. 19. Specific stress-strain curve for Al solid and Al foam samples.

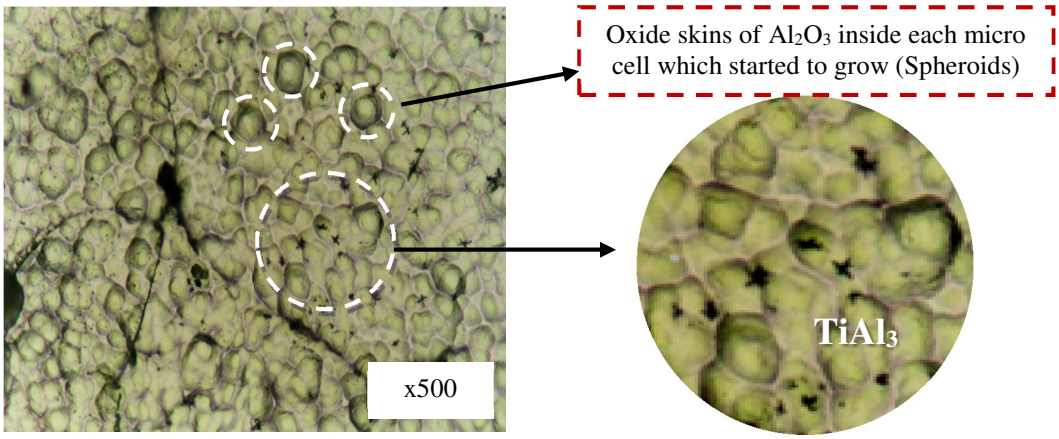

Fig. 20. Microstructure of Al Foam examined under Axiovert microscope with magnification x500 produced with 2% CaCO3.

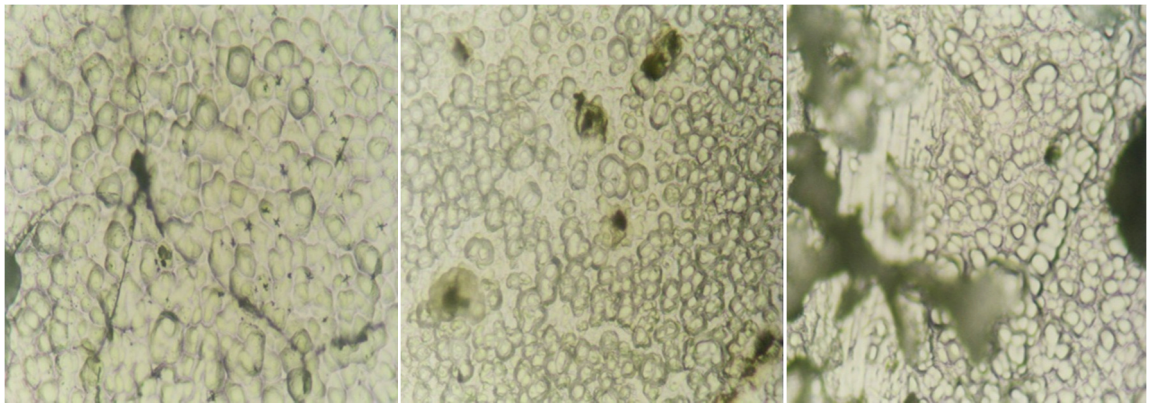

(a) 2% $CaCO_3$ (b) 3% $CaCO_3$ (c) 4% $CaCO_3$

Fig. 21. Structure of Al foam produced with different percentages of $CaCO_3$ (x500).

Table 1. Processing parameters for foam production.

Parameters	Level 1	Level 2	Level 3
Pre Foaming Temperature (°C)	750	800	850
% $CaCO_3$	2%	3%	4%
Foaming duration (min.)	4 min	7 min	10
stirring speed (r.p.m.)	460	730	1280
stirring duration (min.)	1	1.5	2